

Supporting Information for Ferroelectricity and Large Rashba Splitting in Two-Dimensional Tellurium

Yao Wang(王焱)^{1,2}, Zhenzhen Lei(雷珍珍)¹, Jinsen Zhang(张金森)¹, Xinyong Tao(陶新永)¹, Chenqiang Hua(华陈强)^{3,4 *}, and Yunhao Lu(陆贇豪)³

¹ *College of Materials Science and Engineering, Zhejiang University of Technology, Hangzhou, 310014, China*

² *Moganshan Research Institute at Deqing County Zhejiang University of Technology, Huzhou, 313000, China*

³ *School of physics, Zhejiang University, Hangzhou, 310027, China*

⁴ *Zhongfa Aviation Institute of Beihang University, Hangzhou, 310023, China*

* Corresponding author. E-mail address: huachenqiang@zju.edu.cn

SI Note I:

For Abm2 space group of FE phase, the corresponding point group symmetry is C_{2v} here, which includes 2-fold rotation symmetry of the z-axis and mirror symmetry of [110]-direction. This mirror symmetry constrains the direction of polarization field, which directly leads to the spin polarization with only S_z component, according to the Rashba toy model below:

$$H \propto (\vec{E} \times \mathbf{k}) \cdot \sigma,$$

where \vec{E} and σ represent the electric field and spin Pauli matrix, respectively. As discussed in the main text, FE phase possess the in-plane polarization field and thus the above Hamiltonian can be written as $\{\sigma_z(-E_{x'}k_y) - \sigma_y(-E_{x'}k_z)\}$. For simplicity, we assume that the polarization field is parallel to x' -axis and thus $E_{x'}$ terms are left in the Hamiltonian. For 2D materials, the k_z momentum is meaningless and thus the system will only keep S_z component, i.e., $\sigma_z(-E_{x'}k_y)$. Therefore, near CBM, the spin Hall conductivity can be reasonably calculated according to Eq. (3) in the main text. More interestingly, the spin can be reversed when the direction of $E_{x'}$ (polarization

field) is reversed through the FE phase transition. Such analyses based on the Rashba toy model capture the key characteristics of the DFT results in Figs. 5 and S7.

SI Note II:

Here we will simply discuss the Dresselhaus and Zeeman-type splitting in our FE system. For 2D system, the Dresselhaus contribution normally writes as:

$$H \propto k_x \sigma_x - k_y \sigma_y,$$

from which we will find in-plane spin components (S_x/S_y). But for the FE phase here, the system has only in-plane polarization and S_x/S_y are found to be zero (Fig. S8) near CBM. Thus, we rationally exclude the Dresselhaus contribution near CBM.

For Zeeman-type splitting, the spin-degenerate pair will split mostly in energy not in k -momentum and each band carries the opposite spin component. As shown in Figs. 5 and S8, near band edge, the key feature of FE system is the k -momentum band-splitting, quite different from the Zeeman-type bands. Therefore, we also exclude the Zeeman-type contribution near CBM.

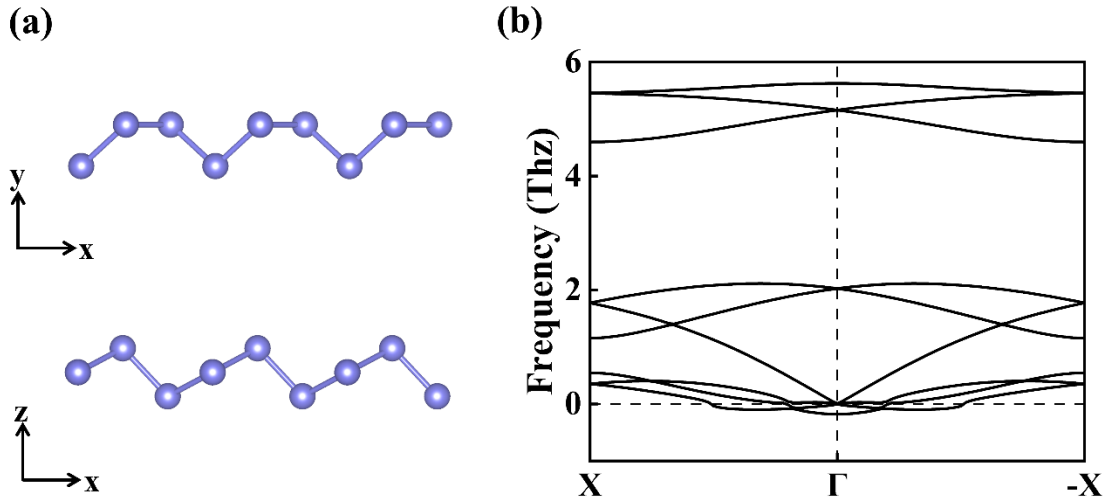


Fig. S1. (a) Top view and side view of 1D α -Te. (b) The phonon spectrum of 1D α -Te with one imaginary chiral-rotation mode at Γ .

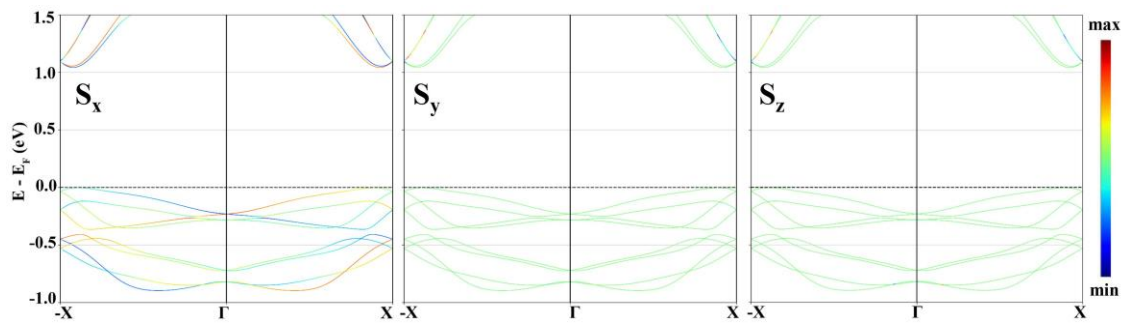


Fig. S2. Spin-resolved bands of 1D s-Te.

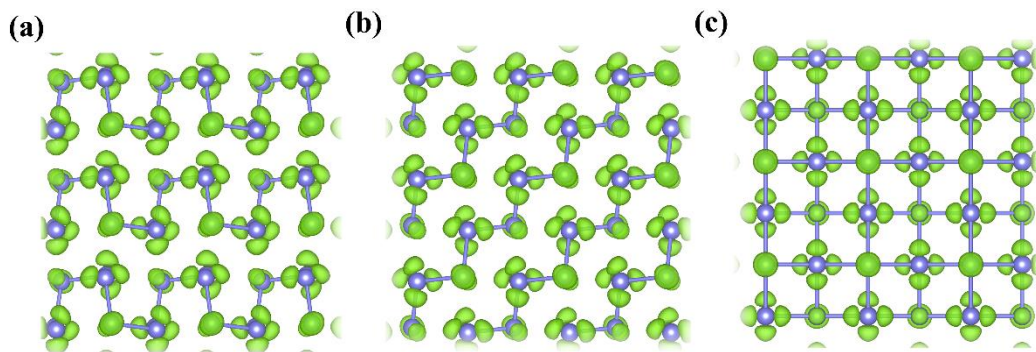


Fig. S3. ELF distribution of (a) phase A, (b) phase C and (c) phase B. The isosurface is 0.9 e/Bhor^3 .

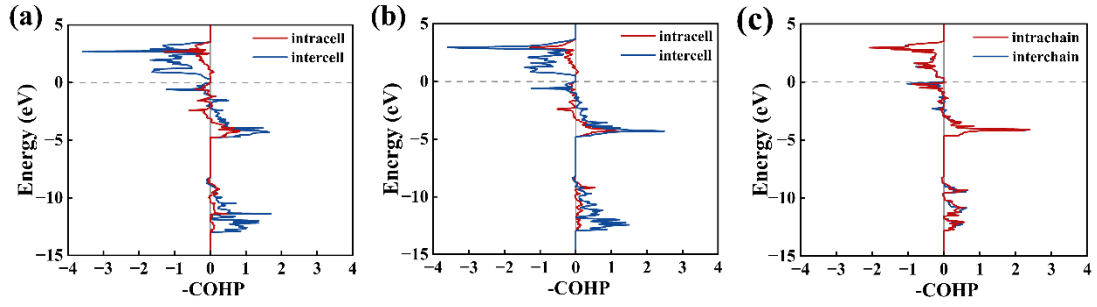


Fig. S4. COHP results. (a)–(b) intra/inter-cell interactions for phase A and C, respectively. (c) Intra/inter-chain interactions for the phase B.

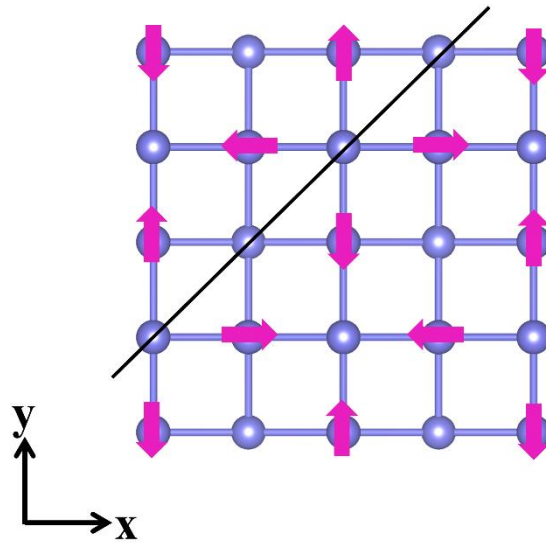


Fig. S5. The schematic figure of vibration mode λ_4 . The black line denotes the remaining Te-chain after the distortion. Such structure is unstable during optimization, and it will transition back to phase B.

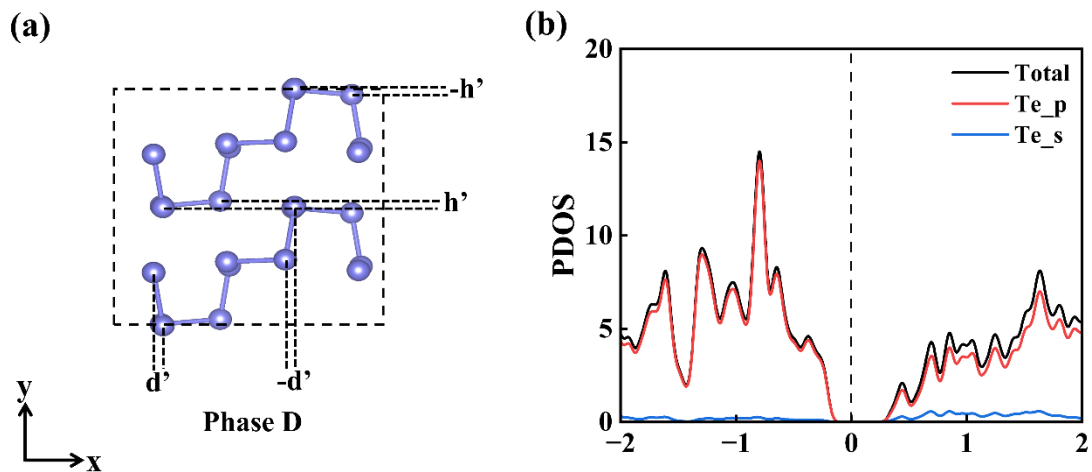


Fig. S6. (a) Top view of phase D in a $2 \times 1 \times 1$ supercell. (b) Partial density of states for phase D, exhibiting the semiconducting behavior.

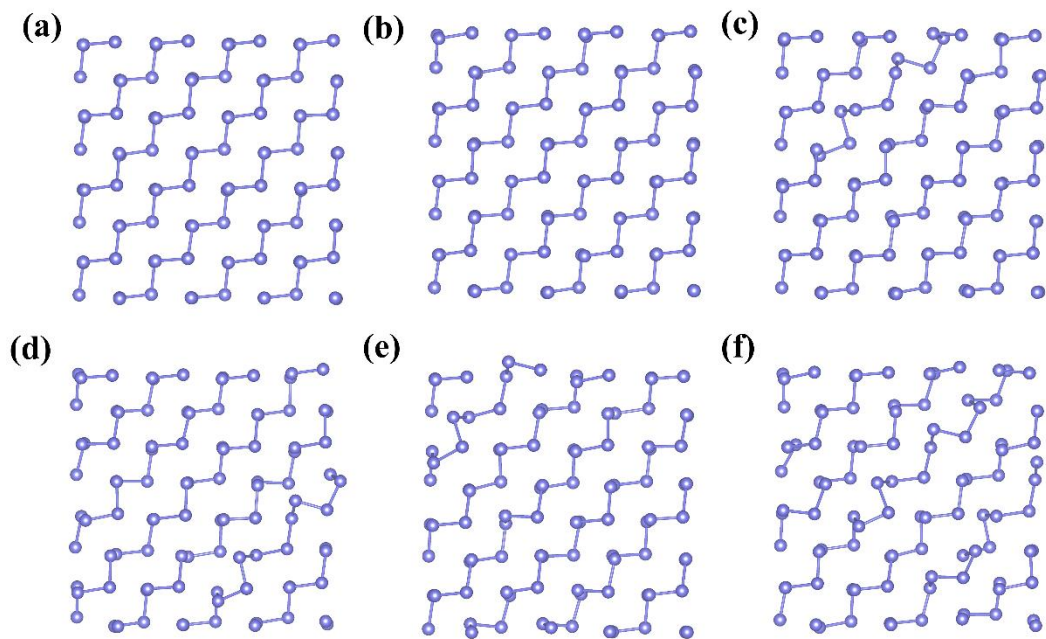


Fig. S7. AIMD results of phase C structure at different temperatures: (a) 20 K, (b) 30 K, (c) 40 K, (d) 50 K, (e) 60 K and (f) 70 K.

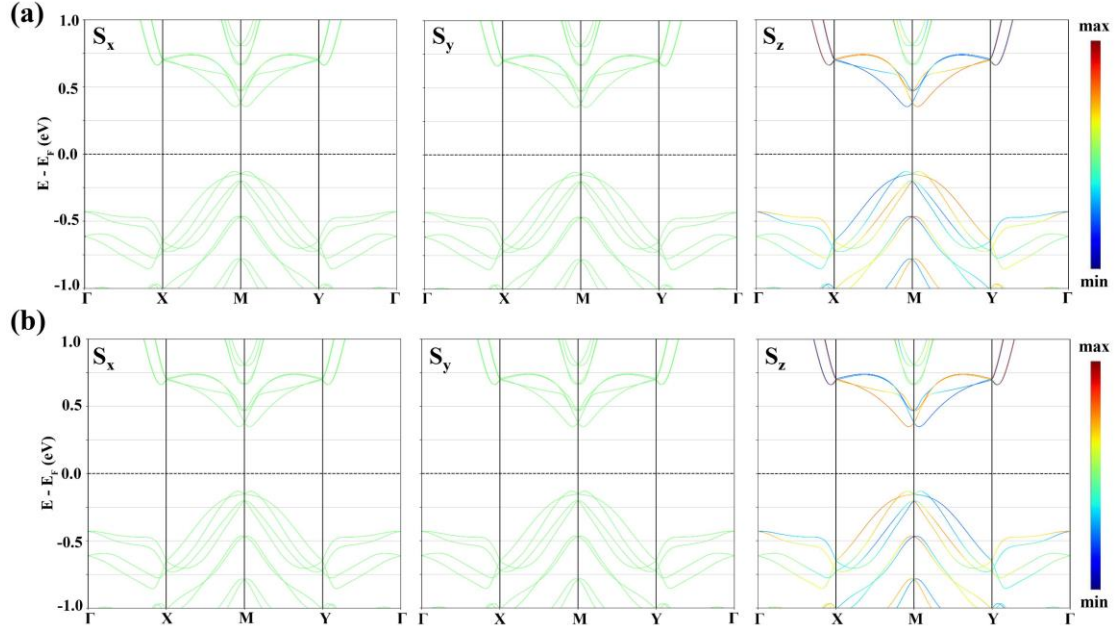


Fig. S8. (a)–(b) Band structures of phase C and C', respectively. The spin components are projected. S_x and S_y components are found to be zero. It is obvious to see that the spin polarization is reversed for phase C and C', according well with the toy model.

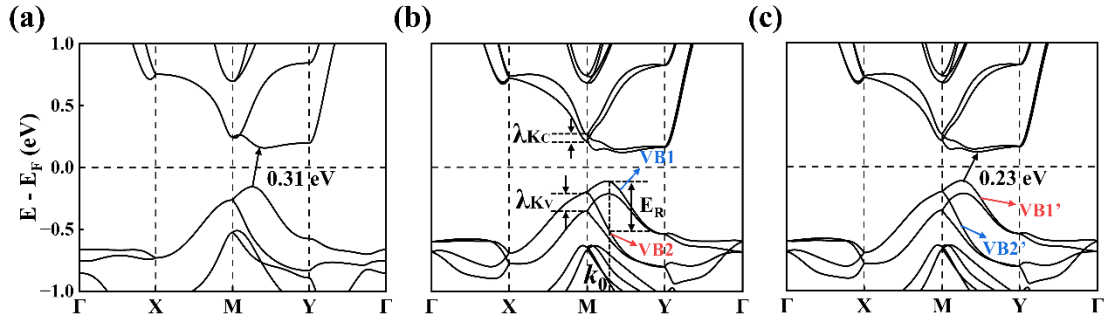


Fig. S9. (a) Band structure of A/A' phases without SOC. (b)–(c) Band structures of A/A' phases with SOC, respectively. Under phase transition from A to A', the spin polarization reverses near VBM and CBM.